Thin Solid Films 559 (2014) 64–68

Contents lists available at ScienceDirect

Thin Solid Films

journal homepage: www.elsevier.com/locate/tsf

Ultra-thin oxide films for band engineering: design principles and numerical experiments ☆

Keith T. Butler *, Aron Walsh

Centre for Sustainable Chemical Technologies, Department of Chemistry, University of Bath, Claverton Down, Bath BA2 7AY, UK

ARTICLE INFO

Available online 28 October 2013

Keywords:
Conducting oxides
Band engineering
Photovoltaics
Ultra-thin films
Dipole layer

ABSTRACT

The alignment of band energies between conductive oxides and semiconductors is crucial for the further development of oxide contacting layers in electronic devices. The growth of ultra thin films on the surface of an oxide material can be used to introduce a dipole moment at that surface due to charge differences. The dipole, in turn, alters the electrostatic potential — and hence the band energies — in the substrate oxide. We demonstrate the fundamental limits for the application of thin-films in this context, applying analytical and numerical simulations, that bridge continuum and atomistic. The simulations highlight the different parameters that can affect the band energy shifting potential of a given thin-film layer, taking the examples of MgO and SnO_2. In particular we assess the effect of formal charge, layer orientation, layer thickness and surface coverage, with respect to their effect on the electrostatic potential. The results establish some design principles, important for further development and application of thin-films for band energy engineering in transparent conductive oxide materials.

1. Introduction

Traditional design of transparent conducting oxides (TCOs) for technological application has concentrated on engineering the optical absorption and the electronic conductivity, through doping and defect chemistry [1–5]. Increasingly it is becoming important to optimise different parameters in order to realise the potential of TCOs in new technological applications. In the context of thin-film photovoltaics the interface between TCOs and semiconductors is of great importance. For optimal device performance and lifetimes it is necessary to form a stable interface between the TCO and the semiconductor, it is also necessary to have an appropriate alignment of the electronic energy levels across the interface.

The alignment of the electronic energy levels is the so called band alignment and is analogous to the Schottky barrier formed at metal–semiconductor interfaces [6,7] in traditional semiconductor devices. The Schottky barrier contributes to the contact resistance (depending on doping levels) according to the thermionic model [8]:

$$R_c = \frac{k}{qA^*T} exp\left(\frac{q\phi_b}{kT}\right) \quad (1)$$

Here ϕ_b is the Schottky barrier, or band offset in the case of semiconductor–semiconductor interfaces. Usually, the smallest possible band offset is desirable for optimal device performance. Recently a lot of effort has been focused on establishing universal alignments of band energies in important semiconducting materials [4,9–15]. Developing a database of universally aligned energies allows for the prediction of appropriate material combinations for minimal band offsets. In some cases it may be impossible to realise such a combination of band energies for a given semiconductor. It is desirable, therefore, to be able to manipulate the band energies of either the semiconductor, the contact, or both in order to reduce the offset.

Surface dipoles in materials are well known to result in shifting the electrostatic potential, and hence workfunctions, of metals and semiconductors. Indeed, the effect of halide atoms adsorbed onto a metal surface on the metal workfunction was reported in the 1920s by Ives, Langmuir and Becke [16–18] and on Si and Ge semiconductor workfunctions more than 40 years ago [19]. More recently self-assembled monolayers have been used to tune energy levels for organic photovoltaic and organic light emitting diode (OLED) devices [20–22]. The effect of LiF buffer layers in OLED devices has recently been attributed to its dipole forming effects [23]. Modern synthetic techniques, for example molecular beam epitaxy and atomic layer deposition, make the realisation of atomically thin surface layers of one material on another possible. Therefore it is reasonable to envisage the possibility of the growth of an ultra-thin layer of one oxide on the surface of another, resulting in a surface dipole, shifting the band energies in the substrate oxide.

Using Tasker notation [24], oxide surfaces can be split into three categories. Type I: individual layers are charge neutral, no net dipole [e.g. MgO(001)]; type II: individual layers are charged, but groups of layers are charge neutral and non-polar [e.g. Al_2O_3(0001); TiO_2(110)]; type III: groups of layers have a net dipole [MgO(111); $SrTiO_3$(100)].

* Corresponding author.
E-mail address: a.walsh@bath.ac.uk (A. Walsh).

0040-6090/$ – see front matter © 2013 The Authors. Published by Elsevier B.V. All rights reserved.
http://dx.doi.org/10.1016/j.tsf.2013.10.108

Type III surfaces are unstable with respect to chemical or surface reconstructions. In this contribution we consider only thin film growth on type I surfaces. We use these models to establish a number of general design principles, which can be applied to achieve band engineering through surface layer modification. We consider first a simple analytical electrostatic model of a single dipole on the surface of a material, demonstrating the effects of dipole charge and orientation. To bridge between continuum and atomistic theories, we apply an electrostatic simulation of a model consisting of polarisable point charges in a rocksalt structure (MgO) with Parry summation [25] to consider a case closer to the realistic systems. The general principles outlined in this work can be used to inform the selection of potential candidate thin-film layers for band engineering purposes and will serve as a screening for candidate materials combinations for further high level quantum mechanics simulations and experimental synthesis.

2. Models

2.1. Analytical

The ionization potential (IP) is defined as the energy required to remove an electron from the highest energy state in the lattice to the vacuum level. The contributions to the IP can be partitioned, similarly to the workfunction in the work of Bardeen [26], into the binding energy of the electron in the lattice and the energy required to pass through the electrostatic double-layer at the surface. We approximate the electrostatic potential due to the surface layer as resulting from the dipole caused by the ionic charge separation in the oxide capping material. The underlying oxide has a zero net dipole moment in the bulk, due to alternating dipole layers cancelling one another, with only the surface layer potentially contributing to the dipole. Commonly the surface layer can reconstruct to cancel out the dipole [27,28], however polar surfaces are well documented, for example the (0001) surface of wurtzite structured ZnO [29].

In our models we consider the effect of capping a non-polar surface of rutile structured SnO_2. In the case of the non-polar surface the entire dipole electrostatic field will be due to the capping layer. Effects of carrier induced band bending or space-charge formation are not considered.

The separations of the poles in the dipole correspond to the interatomic bonding distances of the constituent ions in the bulk lattice of the capping layer. Having established these criteria we now estimate how the presence of a range of capping materials can bend the electronic bands in SnO_2.

The dipole moment of the surface is

$$\vec{\mathbf{p}} = q\vec{\mathbf{d}} \tag{2}$$

Where $\vec{\mathbf{d}}$ is the ionic separation and q is the absolute value of the charges on the ions. As stated earlier we assume the dipoles to be normal to the surface, therefore the separation only has a z component.

The magnitude of the band bending effect of the dipole is dependent on the dielectric screening of the lattice. For the single dipole scenario, we are interested in the dipole field in a region similar in magnitude to the charge separation which gives rise to the dipole. In this instance the electrostatic potential of the dipole, in the z dimension is

$$V_{Dip}(z) = \frac{1}{4\pi\epsilon^o}\frac{\vec{\mathbf{p}}}{\vec{\mathbf{z}}^2} \tag{3}$$

where ϵ^o is the static dielectric screening of the lattice and $\vec{\mathbf{z}}$ is the distance from the centre of the dipole. The total electrostatic potential of the lattice at a point z is given by

$$V(z) = V_{Lat}(z) + V_{Dip}(z), \tag{4}$$

where $V_{Lat}(z)$ is the bulk macroscopic electrostatic potential of the lattice.

The dielectric screening tensor of SnO_2 is anisotropic, therefore different values of ϵ^o must be used depending on the surface orientation. For the (001) surface, we use $\epsilon^o_{33} = 9.86$ [30].

2.2. Numerical

For consideration of a more realistic arrangement of charges corresponding to a metal halide monolayer on a substrate oxide, we use pairwise interatomic potentials following the Born model as implemented in the General Utility Lattice Program [31] code. We model LiF on the non-polar MgO (001) surface. LiF is commonly employed as an electron blocking layer at both high and low workfunction electrodes [32–35] due to the dramatic improvement of device performance. The point charge models are constructed based on the MgO lattice, which has a cubic structure (space group Fm $\bar{3}$ m) with a lattice constant of 4.212 Å. The MgO region is constructed with charges of +/− 2 e at alternating lattice sites. The LiF layer is represented with charges of +/− 1 e at alternating lattice sites. The MgO crystal is terminated with the non-polar (001) surface and the LiF layer is placed 3 Å above the surface. We simulate the system as a 2D surface and calculate the electrostatic potential using a corrected Parry summation method [25]. In order to account for the charge screening effects of polarisation we represent the O and F ions using a core–shell model [36]. The interactions between the ions are then a combination of short-range Buckingham potentials from the parameter set of Binks [37] and long-range Coulomb interactions. The model reproduces the experimental static and high-frequency dielectric constants of MgO to reasonable accuracy.

3. Results

3.1. Analytical

In the analytical model we first consider a one-dimensional system, with a *single* dipole at one terminal, which could be thought of as an isolated molecule. The electric field of a dipolar molecule is presented in Fig. 1(a). Note that at either side of the dipole centre the electrostatic field decays to a common level; the vacuum level. Also note that immediately to the left of the negative charge the electrostatic potential is increased, whilst to the right of the positive charge the electrostatic field is decreased.

Using the textbook analytical model described we calculate the effect of placing a single dipole on the (001) surface of SnO_2. The material is represented by the zz component of the dielectric tensor. The results for the effect of the magnitude of the polar charges are presented in Fig. 1(b), where we set a distance between the dipolar molecule and the SnO_2 surface ($\vec{\mathbf{z}}$ in Eq. (3)) to 3 Å. With the negative pole of the dipole directed towards the surface, we can obtain a maximum band bending of between −0.4 and −2.1 eV at the surface, depending on the formal charges of the poles, from $q = 1$ to $q = 6$. In this model, the band bending decays with $1/r^2$ and the length of decay is inversely proportional to the dielectric constant of the material.

In addition to considering the effects of charge and separation of the dipole, we now also consider how the orientation of the dipolar species at the surface affects the band bending. Fig. 2 presents the effect of orientation, in this case the formal charges of the dipole poles are $q = \pm 2$ and the separation of the poles is 3 Å. The centre of the dipole remains 3 Å from the centre MgO region, with the poles rotated about the fixed centre, so that the dipole vector forms an angle (γ) with a vector parallel to the surface of the MgO, as illustrated in Fig. 2. For a single dipole on the material surface, the maximum effect is not when the dipole is perpendicular to the surface, but rather occurs at about 45°. These models represent some fundamental limits when considering the effect of single dipolar molecule on a material surface and demonstrate how the arrangement and charge of the dipole layer can affect the band

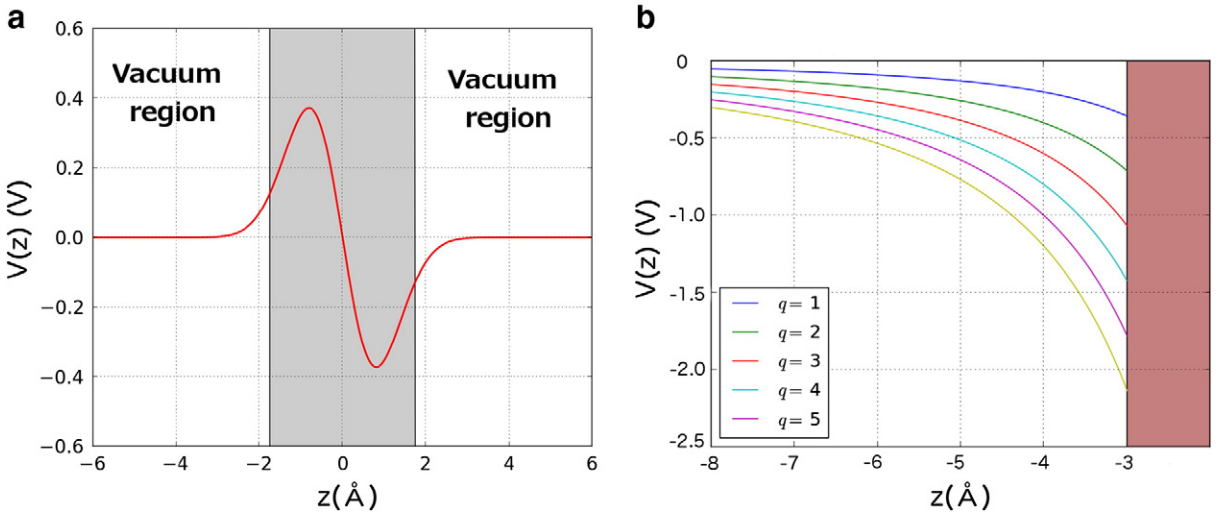

Fig. 1. a) The electrostatic potential due to a single dipolar molecule. b) Band-bending of the SnO_2 valence band (set to 0 V) due to capping of the (001) surface with a molecule of oxide M_xO_y; the value of charge is $q = 2 \times x/y$, and the region containing the dipole is shaded, the unshaded region is the SnO_2.

energies. We will now consider the case where a *continuous* dipole layer is present at a material surface, with direct numerical modelling.

3.2. Numerical

We now increase the dimensionality of the system by considering the effects of a continuous dipole layer at a material surface. The stoichiometric (001) surface of MgO investigated has no macroscopic dipole moment; therefore, we introduce the dipole by inclusion of the layer of differently charged ions (LiF). We consider the effects of orientation, charge layer thickness and percentage of surface coverage.

The effect of a dipole layer extending infinitely in two dimensions is plotted in Fig. 3 in the plane perpendicular to the dipole layer. Similar to the isolated dipole presented above, the electrostatic potential is positive to the left of the negative pole of the sheet and negative to the right of the positive pole of the sheet. However, in contrast to the isolated molecule, the electrostatic field does not decay to the same vacuum level on both sides of the dipole sheet. The dipole sheet introduces a step function in the electrostatic potential; analogous to a parallel-plate capacitor. The step in electrostatic potential across the dipole layer (ΔV) can be calculated through the Helmholtz equation for describing the potential difference across an electric double-layer at a surface [38], which considers a homogeneous plate capacitor formed by a solid surface and the outer end of the dipole layer with a dipole moment density, μ/A:

$$\Delta V = \frac{\mu}{\epsilon_0 A} \tag{5}$$

where ϵ_0 is the permittivity of free space. This relation refers to dipoles only, but could be extended to higher order multipoles.

The case of an infinite dipole sheet is useful for deriving analytical expressions for potentials due to dipole layers; however, in final equilibrium geometries it is less relevant, since it would result in a divergent surface energy [24]; therefore, we should consider how a finite dipole sheet affects the potential. It has been demonstrated [39] that for a finite dipole sheet the potential energy on either side of the dipole sheet decays to a common vacuum level, as in the case of the isolated molecule, and that the length of this decay is related to the area of the dipole sheet. This places an important constraint on the design of dipole layers to be

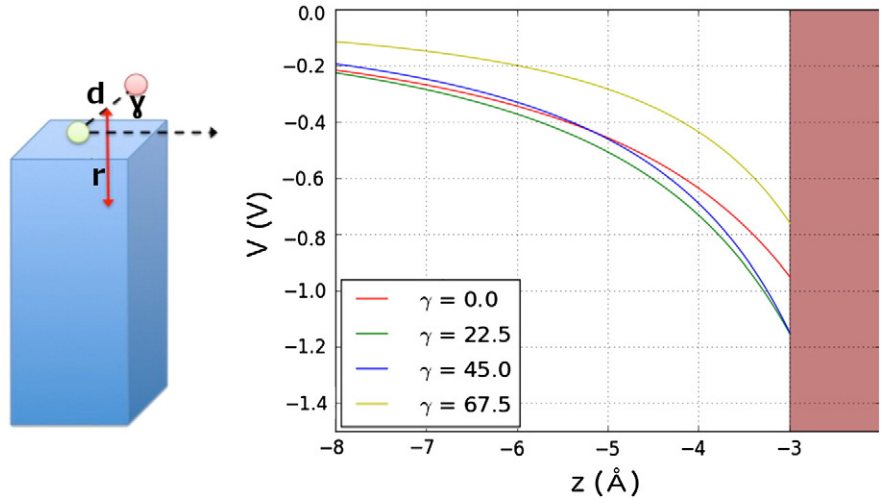

Fig. 2. Left: schematic representation of the molecular orientation of a dipolar molecule at a material surface. The poles of the dipole are represented by circles, separated by a distance d, the dipole moment forms an angle, γ, with the plane of the surface, *r* is the distance from the centre of the dipole to a point in the material. Right: the band-bending on the SnO_2 valence band (set to 0 eV) due to capping of the (001) surface with a monolayer of oxide M_xO_y, demonstrating the effect of different dipole orientations (γ). The value of charge is $q = 2$ and the region containing the dipole is shaded.

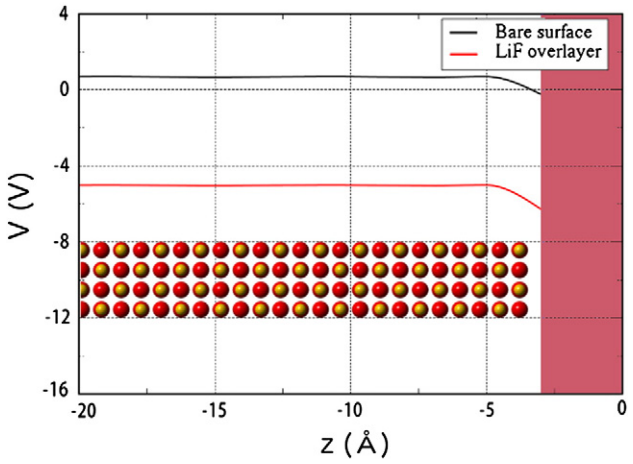

Fig. 3. The effect of an infinitely expended 2D polar sheet of LiF at an MgO surface on the site Madelung potential of O in MgO. The values are shown with reference to the Madelung potential of O in bulk MgO. The bare surface introduces a slight increase in potential and the LiF layer shifts the potential below that of bulk MgO. The MgO region is indicated by the atomic coordinates inset on the graph, the LiF layer is in the shaded region.

grown on materials: the surface dimensions of the dipole layer should be larger than the width of the semiconductor layer in which the band shift is desired. In this section we consider the Madelung potential of the O ions in the oxide. This choice is made since the O states tend to dominate the valence band edge; therefore, any shift in the O electrostatic environment will result in a shift in the band edge.

As was the case for the single dipole, the orientation of the dipole layer has a pronounced effect on the magnitude of band shifting, see Fig. 4. However in this case the maximum effect is for a sheet in which all dipoles are oriented perpendicular to the surface. For the parallel film, there is no macroscopic dipole, with the small shift arising from higher-order multipoles.

The thickness of the dipole layer can also be expected to affect the band bending. For our models we consider a simple layer-by-layer addition to the dipolar material, in which all of the layers have the same dipole orientation. In a real system the inclusion of more layers would result in atomic re-arrangements above a critical threshold; however, as we are primarily interested in establishing a set of limiting factors, we will assume a coherent film. The initial layer of LiF on the MgO surface has a small effect on the electrostatics, as the LiF dipoles are parallel to the MgO surface, which, reduces the potential shift. The effect of increasing the numbers of layers in the dipole layer is a linear increase in the electrostatic potential, hence a linear increase in the band shifting effect of the over-layer. This follows the analytical model, as the number of layers is increased the internal dipoles cancel one another; therefore the thickness increases the terminal separation and the macroscopic dipole strength, as described by Eq. (2). The linear increase in the electrostatic potential energy of the system, such as presented in Fig. 5, cannot prevail indefinitely and at a certain critical point the energy penalty for the dipole layer will exceed the energy of atomic rearrangement required to cancel the dipole; the so-called polarisation catastrophe [40]. This represents a fundamental limit on how thick the dipole layer can be in order to avoid compensating chemical changes in the system.

So far all of the scenarios we have considered have represented a total coverage of the substrate surface by the dipole inducing material. Under synthesis conditions generally only a fractional coverage of the material surface will be realisable. Therefore, we now consider how the percentage of the surface covered will affect the band energies. We have constructed models with 3 layers of LiF, at 15° to the surface, covering 0, 6.25, 11, 25 and 100% of the MgO surface, the results of these simulations are presented in Fig. 6. There is a strong linear correlation between the effect of the percentage coverage and the potential shift, and this correlation continues to complete coverage. This is an important consideration, since it allows us to extrapolate from calculated values of potential shift at high coverage to more experimentally realistic levels, allowing the establishment of minimum coverage criteria from more accurate first-principles calculations, in appropriate boundary conditions.

The results demonstrate that the single most important factor affecting the electrostatic potential is the orientation of the dipole layer, therefore designing a layer with the right geometry will be important for achieving the desired potential shift. In case it is not possible to achieve the desired angle of the dipole layer at the surface then a degree of control is offered by altering the thickness of the surface layer, this perturbation increases linearly with the number of atomic layers.

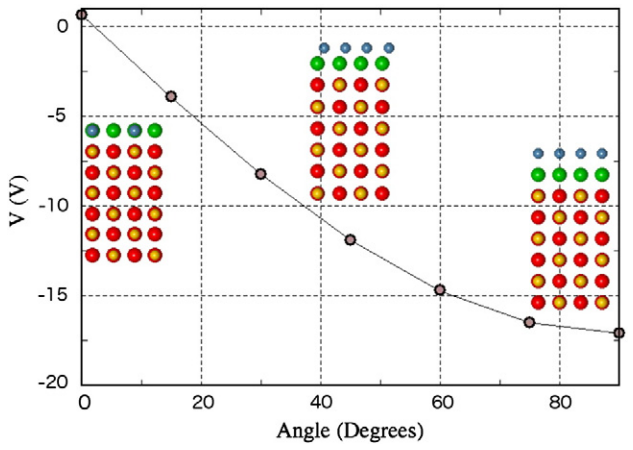

Fig. 4. The effect of angular orientation of the LiF layer on the O site Madelung potential in MgO relative to the bulk potential. The angle on the abscissa is the angle formed between the dipole moment vector and the plane of the surface. The insets show the atomic positions across the interface at various orientations, with yellow = Mg, red = O, green = F, blue = Li.

4. Conclusions

In this contribution we have considered the possibility of using thin films of materials to induce surface dipoles on oxide materials, resulting in a shifting of the electrostatic potential of the oxide and a shifting of the band energies. Using a combination of analytical and numerical modelling we have investigated the effects of charge, orientation, thickness and surface coverage on the band energies. The results show that

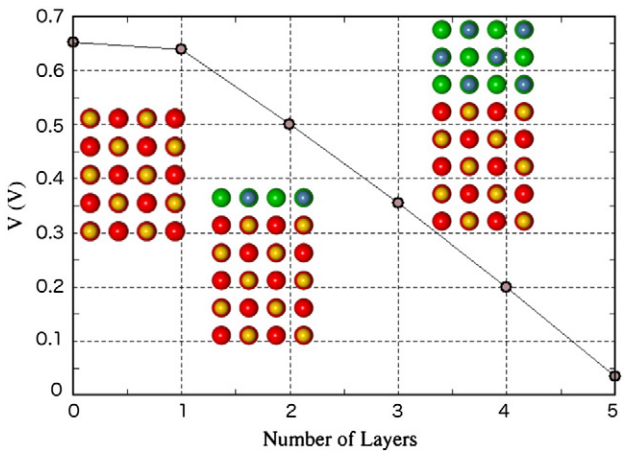

Fig. 5. The effect of number of layers of the LiF on the O site Madelung potential in MgO relative to the bulk potential.

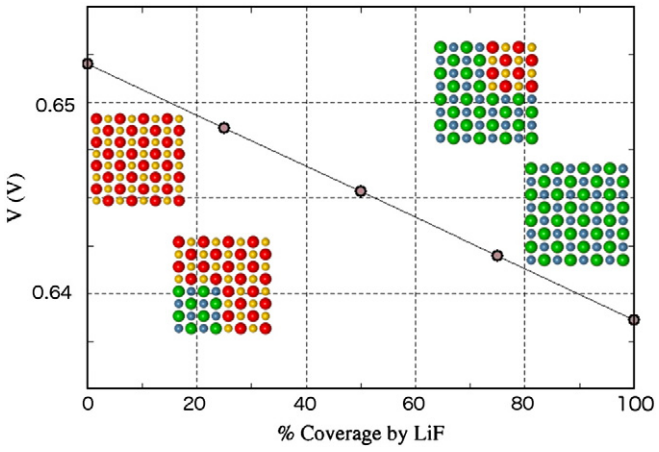

Fig. 6. The effect of surface coverage of MgO by a (sub-)monolayer LiF with an orientation of 15° on the O site Madelung potential in MgO relative to the bulk potential. The insets show the MgO surface with 0, 25, 75 and 100% coverage from above the surface.

the orientation of the surface layer has a large bearing on how large the dipole effect will be. Factors such as thickness of the layer and surface coverage have smaller, but still significant effects on the potential. The results of these models can be used to establish some general design rules for the use of thin films to engineer band energies and provide motivation of further studies at higher levels of theory to establish quantitative predictions.

Acknowledgments

We acknowledge A. A. Sokol and J. H. Harding for useful discussions. The work was funded by EPSRC (Grant Nos. EP/F067496 and EP/J017361/1) through the HPC Materials Chemistry Consortium and the SUPERSOLAR Hub.

References

[1] D.S. Ginley, H. Hosono, D.C. Paine, Handbook of Transparent Conductors, 1st ed. Springer, New York, 2010.
[2] S. Lany, A. Zunger, Phys. Rev. Lett. 98 (2007) 045501.
[3] A.A. Sokol, S.A. French, S.T. Bromley, C.R.A. Catlow, H.J.J. van Dam, P. Sherwood, Faraday Discuss. 134 (2007) 267.
[4] Y.-H. Li, A. Walsh, S. Chen, W.-J. Yin, J.-H. Yang, J. Li, J.L.F. Da Silva, X.G. Gong, S.-H. Wei, Appl. Phys. Lett. 94 (2009) 212109.
[5] A. Walsh, J.L.F.D. Silva, S.-H. Wei, J. Phys. Condens. Matter 23 (2011) 334210.
[6] W. Schottky, Phys. Z. 41 (1940) 570.
[7] J. Bardeen, Phys. Rev. 71 (1947) 717.
[8] V. Rideout, Solid State Electron. 18 (1975) 541.
[9] S.B. Zhang, S.-H. Wei, A. Zunger, J. Appl. Phys. 83 (1998) 3192.
[10] S.B. Zhang, S.-H. Wei, A. Zunger, Phys. Rev. Lett. 84 (2000) 1232.
[11] C.G. van de Walle, J. Neugebauer, Nature 423 (2003) 626.
[12] A. Walsh, C.R.A. Catlow, R. Galvelis, D.O. Scanlon, F. Schiffmann, A.A. Sokol, S.M. Woodley, Chem. Sci. 3 (2012) 2565.
[13] K.T. Butler, P.E. Vullum, A.M. Muggerud, E. Cabrera, J.H. Harding, Phys. Rev. B 83 (2011) 235307.
[14] K.T. Butler, J.H. Harding, Phys. Rev. B 86 (2012) 245319.
[15] L.A. Burton, A. Walsh, Appl. Phys. Lett. 102 (2013) 132111.
[16] H.E. Ives, Astrophys. J. 60 (1924) 209.
[17] I. Langmuir, K.H. Kingdon, Proc. Phys. Soc. Lond. Sect. B 61 (1925) A107.
[18] J.A. Becker, Phys. Rev. 28 (1926) 341.
[19] R. Weber, W. Peria, Surf. Sci. 14 (1969) 13.
[20] C.-T. Tseng, Y.-H. Cheng, M.-C.M. Lee, C.-C. Han, C.-H. Cheng, Y.-T. Tao, Appl. Phys. Lett. 91 (2007) 233510.
[21] B. de Boer, A. Hadipour, M. Mandoc, T. van Woudenbergh, P. Blom, Adv. Mater. 17 (2005) 621.
[22] Y. Zhou, C. Fuentes-Hernandez, J. Shim, J. Meyer, A.J. Giordano, H. Li, P. Winget, T. Papadopoulos, H. Cheun, J. Kim, M. Fenoll, A. Dindar, W. Haske, E. Najafabadi, T.M. Khan, H. Sojoudi, S. Barlow, S. Graham, J.-L. Brdas, S.R. Marder, A. Kahn, B. Kippelen, Science 336 (2012) 327(http://www.sciencemag.org/content/336/6079/327.full.pdf).
[23] T. Aytun, A. Turak, I. Baikie, G. Halek, C.W. Ow-Yang, Nano Lett. 12 (2012) 39(http://pubs.acs.org/doi/pdf/10.1021/nl202838a).
[24] P.W. Tasker, J. Phys. C Solid State Phys. 12 (1979) 4977.
[25] D. Parry, Surf. Sci. 49 (1975) 433.
[26] J. Bardeen, Phys. Rev. 49 (1936) 653.
[27] R. Nosker, P. Mark, J. Levine, Surf. Sci. 19 (1970) 291.
[28] O. Dulub, U. Diebold, G. Kresse, Phys. Rev. Lett. 90 (2003) 016102.
[29] M. Kunat, S. Gil Girol, T. Becker, U. Burghaus, C. Wöll, Phys. Rev. B 66 (2002) 081402.
[30] D. Roessler, W. Albers Jr., J. Phys. Chem. Solids 33 (1972) 293.
[31] J.D. Gale, A.L. Rohl, Mol. Simul. 29 (2003) 291(http://www.tandfonline.com/doi/pdf/10.1080/0892702031000104887).
[32] J.M. Zhao, S.T. Zhang, X.J. Wang, Y.Q. Zhan, X.Z. Wang, G.Y. Zhong, Z.J. Wang, X.M. Ding, W. Huang, X.Y. Hou, Appl. Phys. Lett. 84 (2004) 2913.
[33] Y. Zhao, S. Liu, J. Hou, Thin Solid Films 397 (2001) 208.
[34] C.J. Brabec, S.E. Shaheen, C. Winder, N.S. Sariciftci, P. Denk, Appl. Phys. Lett. 80 (2002) 1288.
[35] D. Grozea, A. Turak, X.D. Feng, Z.H. Lu, D. Johnson, R. Wood, Appl. Phys. Lett. 81 (2002) 3173.
[36] B.G. Dick, A.W. Overhauser, Phys. Rev. 112 (1958) 90.
[37] D.J. Binks, R.W. Grimes, Solid State Commun. 89 (1994) 921.
[38] S. Srinivasan, Fuel Cells, Springer, US, 2006, p. 27.
[39] G. Heimel, I. Salzmann, S. Duhm, N. Koch, Chem. Mater. 23 (2011) 359(http://pubs.acs.org/doi/pdf/10.1021/cm1021257).
[40] N. Nakagawa, H.Y. Hwang, D.A. Muller, Nat. Mater. 5 (2006) 204.